Effects of the Intramode-Group Coupling Induced by the Elliptical Deformation of Orbital Angular Momentum Fibers

Hu Zhang, *Member, IEEE*, Hui Li, Xiaoguang Zhang, *Member, IEEE*, Jingxuan Yang, Ze Chen, Lixia Xi, Wenbo Zhang, and Xianfeng Tang

***Abstract*—Based on the coupling mode theory and numerical simulation, intramode-group coupling in orbital angular momentum (OAM) fibers with elliptical deformation is analyzed in depth. The elliptical deformation not only introduces a time delay difference between even and odd modes of the same high-order vector mode but also destroys the structure of the high-order vector modes; the structural damage depends on the strength of the elliptical deformation. When the elliptical deformation is relatively small, the structural damage of high-order vector modes can be ignored and coupling can be thought as occurring only between two OAM modes composed of the same high-order vector mode. While the elliptical deformation becomes larger, the structural damage cannot be ignored, coupling appears among four OAM modes in the same OAM mode group, and the coupling between two OAM modes composed of the same high-order vector mode is more serious. The results will pave the way for the establishment of accurate propagation models and the optimization of the OAM fiber design.**

***Index Terms*—Optical fiber communication, mode division multiplexing (MDM), orbital angular momentum (OAM), mode coupling.**

I. Introduction

TO SOLVE the pending capacity crunch of optical fiber communication in the next decades, mode division multiplexing (MDM) is considered a promising method to overcome the capacity bottleneck imposed by the nonlinear Shannon limit in the single-mode fiber [1]–[4]. Traditional MDMs are implemented by transmitting multiple orthogonal linearly polarized (LP) modes in the few-mode fibers (FMFs), which increase the system capacity in proportion to the number of modes. However, because the LP modes in these weakly-guiding fibers have small effective index separation, coupling is severe among these modes [5], [6]. The mode coupling can be addressed using the multiple-input-multiple-output (MIMO) digital signal processing [7], which will undoubtedly increase the complexity and cost of the system. A scheme to solve this problem is to suppress the mode coupling by optimizing the fiber structure. Recently, two types of optical fibers have been proposed to mitigate mode coupling, which simplify or eliminate the MIMO processing. One type is elliptical-core fibers (ECFs) to support linearly polarized vector (LPV) modes [8], [9], and the other is ring-core fibers to support orbital angular momentum (OAM) modes [10]–[12]. Compared to the former, the latter can support more modes and provide a larger communication capacity. Here, we focus on the latter.

The prerequisite for implementing free-MIMO processing in an OAM-MDM system is that there is no coupling among the OAM modes in fibers, or the coupling is very weak and can be ignored. Therefore, it is of great importance to grasp the coupling mechanism of OAM modes and subsequently design OAM fibers to avoid mode coupling. Mode coupling in OAM fibers has two sources: intrinsic mode coupling and extrinsic mode coupling. The former comes from the spin-orbit coupling caused by a large index contrast between the core and the cladding of OAM fibers, which has been thoroughly investigated, and great research results have been achieved [13], [14]. The latter originates from geometrical deformations, stress birefringence, bending, twisting, exterior electromagnetic fields, etc. [15]–[20]. OAM modes in fibers are formed by the superposition of even and odd modes from the same high-order vector modes (HE_{l+1} or EH_{l-1} modes) with a phase difference of $\pi/2$. Ideally, the even and odd modes are degenerate; thus, OAM modes can stably exist. However, the degeneracy of modes will be broken, and the eigenmode structure will also be destroyed due to manufacturing defects and extrinsic disturbances. The fiber imperfections will cause different types of OAM mode coupling: (i) coupling between two OAM modes composed of the same high-order vector modes; (ii) coupling among the OAM modes supported by HE_{l+1} and EH_{l-1} modes; (iii) coupling among OAM modes in different OAM mode groups. In the OAM fibers, OAM modes in different mode groups have large effective index separation ($>10^{-3}$) [22];

Manuscript received September 25, 2021; revised October 19, 2021; accepted October 21, 2021. Date of publication October 27, 2021; date of current version November 17, 2021. This work was supported in part by the Fund of State Key Laboratory of IPOC (BUPT) under Grants IPOC2020ZT07 and IPOC2019ZZ02, China, in part by Fund of State Key Laboratory of Advanced Optical Communication Systems and Networks under Grant 2021GZKF008, China, and in part by the National Natural Science Foundation of China under Grants 62075015, 61527820, and 61571057. *(Corresponding authors: Hu Zhang; Hui Li.)*

Hu Zhang, Xiaoguang Zhang, Jingxuan Yang, Ze Chen, Lixia Xi, and Xianfeng Tang are with the State Key Laboratory of Information Photonics and Optical Communications, Beijing University of Posts and Telecommunications, Beijing 100876, China (e-mail: zhh309@bupt.edu.cn, zhh309@sina.com; xgzhang@bupt.edu.cn; yangjingxuan@bupt.edu.cn; zechen2019@163.com; xilixia@bupt.edu.cn; tangxianfengbupt@bupt.edu.cn).

Hui Li is with the Beijing Smart-Chip Microelectronics Technology Company Limited, Beijing 102200, China (e-mail: lihui1206@bupt.edu.cn).

Wenbo Zhang is with the School of Sciences, Beijing University of Posts and Telecommunications, Beijing 100876, China (e-mail: zhangwb@bupt.edu.cn).

Digital Object Identifier 10.1109/JPHOT.2021.3122794

thus, this type of coupling is weak and can be ignored. Therefore, the research is focused on the coupling between modes in the same OAM mode group, which is called the intramode-group coupling. Both (i) and (ii) belong to intramode-group coupling. Here, we take elliptical deformation as an example to analyze the intramode-group coupling in OAM fibers.

In practice, some researchers have preliminarily investigated the OAM mode coupling caused by disturbances [15]–[20]. Yang Yue noted that elliptical deformation would introduce a time delay difference between even and odd modes of HE_{l+1} or $EH_{l\text{-}1}$ modes [15]. Then, Lixian Wang first proposed the concept of "OAM polarization mode dispersion (PMD)" and generalized the form describing the PMD in a single mode fiber to rewrite OAM-PMD in OAM fibers [16]. They laid a foundation for the research of OAM mode coupling; however, the conclusion that perturbations only introduce the effective refractive index difference between even and odd modes is incomplete because they do not consider the structural damage of eigenmodes. As a consequence, they can only analyze the coupling between two OAM modes composed of the same high-order vector modes. Ramesh Bhandari investigated the spatial OAM modal crosstalk by using analytic expressions for a slightly elliptical fiber under the weakly guiding approximation [21]. In addition, the Gianluca Guerra team theoretically analyzed the coupling between OAM modes by adopting the coupled mode equation [23], [24]. The corresponding coupling model is built by applying multimode fiber techniques and taking the OAM modes as basis functions [25], [26]. Based on this theory, the coupling between OAM modes supported by the HE_{l+1} and $EH_{l\text{-}1}$ modes has been investigated, which is of great significance. Mai Banawan *et al.* proposed a coupling model based on numerical mode solver outputs of perturbation to quantify the coupling and degeneracy of OAM modes in OAM fibers [27]. However, the coupling between two OAM modes composed of the same vector modes has still not been analyzed, and the two types of coupling in the same OAM mode group cannot be simultaneously fully considered.

In this paper, we will comprehensively analyze the intramode-group coupling based on high-order vector modes that constitute OAM modes. We first analyze the coupling between high-order vector modes and subsequently elucidate the coupling mechanism between OAM modes in the same OAM mode group. Thus, the paper is structured as follows. In Section II, we present the high-order vector modes and OAM modes in ideal OAM fibers. In Section III, we analyze the coupling between high-order vector modes by coupled-mode theory and numerical simulation. The evidence shows that the elliptical deformation introduces an effective index difference between even and odd modes and destroys the structure of eigenmodes. Different strengths of elliptical deformation cause different structural damages. When the elliptical deformation is small, the structural damage of eigenmodes can be ignored, and the eigenmodes exhibit high mode purity. While the elliptical deformation becomes larger, the structural damage of eigenmodes cannot be ignored, and the eigenmodes of fibers become a hybrid state of HE_{l+1} and $EH_{l\text{-}1}$ modes. In Section IV, we assess the coupling between OAM modes in the same OAM mode group. For OAM fibers with a very small elliptical deformation, coupling occurs between two OAM modes composed of the same vector modes. However, when the elliptical deformation becomes larger, coupling appears among four OAM modes in the same mode group, and the coupling between two OAM modes composed of the same high-order vector mode is more serious. Finally, we draw the conclusions.

II. The Modes of the Ideal OAM Fibers

In general, the fibers supporting OAM modes exhibit a high index contrast between core and cladding. Therefore, the weakly guiding approximation is no longer adopted to achieve the exact eigenstate solutions. The electric field components E_r, E_φ and E_z of eigenmodes in cylindrical coordinates can be obtained by solving Helmholtz equation precisely [28]. To analyze the polarization information of modes in the following, E_r and E_φ components are converted into E_x and E_y components. The eigenmodes with the same orders can be expressed as follows:

$$
\begin{aligned}
HE_{l+1,m}^{even}\begin{pmatrix}E_x\\E_y\\E_z\end{pmatrix}&=\begin{pmatrix}-F_{l,m}(r)\cos l\varphi\\G_{l,m}(r)\sin l\varphi\\-iH_{l,m}(r)\cos(l+1)\varphi\end{pmatrix}e^{i\left(\beta_l^{HE}z-\omega t\right)}\\
HE_{l+1,m}^{odd}\begin{pmatrix}E_x\\E_y\\E_z\end{pmatrix}&=\begin{pmatrix}-F_{l,m}(r)\sin l\varphi\\-G_{l,m}(r)\cos l\varphi\\-iH_{l,m}(r)\sin(l+1)\varphi\end{pmatrix}e^{i\left(\beta_l^{HE}z-\omega t\right)}\\
EH_{l-1,m}^{even}\begin{pmatrix}E_x\\E_y\\E_z\end{pmatrix}&=\begin{pmatrix}F_{l,m}(r)\cos l\varphi\\G_{l,m}(r)\sin l\varphi\\-iH_{l,m}(r)\cos(l-1)\varphi\end{pmatrix}e^{i\left(\beta_l^{EH}z-\omega t\right)}\\
EH_{l-1,m}^{odd}\begin{pmatrix}E_x\\E_y\\E_z\end{pmatrix}&=\begin{pmatrix}F_{l,m}(r)\sin l\varphi\\-G_{l,m}(r)\cos l\varphi\\-iH_{l,m}(r)\sin(l-1)\varphi\end{pmatrix}e^{i\left(\beta_l^{EH}z-\omega t\right)}
\end{aligned}
\tag{1}
$$

where the superscripts "even" and "odd" denote even and odd eigenmodes, respectively; subscripts l ±1 and m are the angular and radial order of the eigenmodes, respectively; $F_{l,\mathrm{m}}$(r), $G_{l,\mathrm{m}}$(r) $H_{l,\mathrm{m}}$(r) are the radial-dependent function of x, y and z directions, respectively; φ is the azimuth angle; β_l^{HE} and β_l^{EH} are the propagation constants of the HE_{l+1} and $EH_{l\text{-}1}$ modes, respectively.

The OAM modes in fibers are formed by superposing degenerate even and odd modes of the same high-order vector modes with a phase difference of $\pm\pi/2$. Due to the large index difference (corresponding to strongly guiding fibers), the synthesized OAM mode is no longer a pure mode with single topological charge number [14], [23]. Thus, the transverse components of OAM modes can be written as follows:

$$
\begin{aligned}
OAM_{\pm l,m}^{+}&=f_{l+1}(r)(\hat{x}\pm i\hat{y})e^{\pm il\varphi}e^{i\left(\beta_l^{HE}z-\omega t\right)}\\
&\quad+g_{l+1}(r)(\hat{x}\mp i\hat{y})e^{\pm i(l+2)\varphi}e^{i\left(\beta_{l+2}^{EH}z-\omega t\right)}\\
OAM_{\pm l,m}^{-}&=f_{l-1}(r)(\hat{x}\mp i\hat{y})e^{\pm il\varphi}e^{i\left(\beta_l^{EH}z-\omega t\right)}\\
&\quad+g_{l-1}(r)(\hat{x}\pm i\hat{y})e^{\pm i(l-2)\varphi}e^{i\left(\beta_{l-2}^{HE}z-\omega t\right)}
\end{aligned}
\tag{2}
$$

where the signs in the superscripts "+" and "−" corresponding to $\hat{x}\pm i\hat{y}$ denote right and left circular polarizations, respectively. Radial function $f_{l\pm1}$(r) and $\mathrm{g}_{l\pm1}$(r) depend on $F_{l,\mathrm{m}}$(r) and

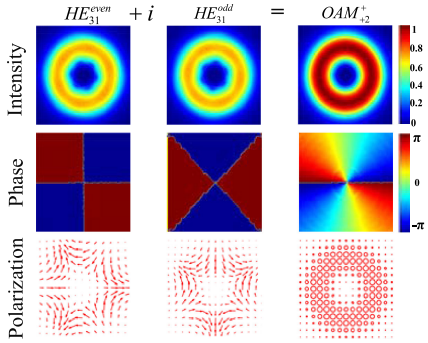

Fig. 1. Intensity, phase and polarization of $OAM^{+}{}_{+2}$ modes.

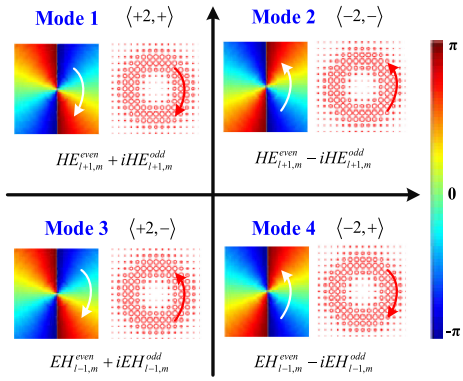

Fig. 2. Composition method of four OAM modes from the OAM mode group for $l = 2$.

$G_{l,\mathrm{m}}(\mathrm{r})$. OAM mode is composed of the dominant component with the helical phase factor exp $(\pm il\varphi)$ and the secondary component with the helical phase factor exp $[\pm i(l \pm 2)\varphi]$. In order to facilitate demultiplexing, we generally take the radial index m as 1, which is omitted in the following. To better understand OAM modes, Fig. 1 explains the process of synthesizing the dominant component OAM_{+2}^{+} mode. The OAM mode exhibits a ring intensity distribution and carries a helical phase wavefront and a circular polarization state.

Not considering the waveguide structure characteristic, the combination form of four OAM modes from the OAM mode group for $l = 2$ is shown in Fig. 2. The white arrows indicate the wavefront rotation direction, and the red arrows is the direction of polarization. For the OAM modes composed of the HE_{l+1} mode, the wavefront rotation direction is aligned with the circular polarization, while for the OAM modes composed of the $EH_{l\text{-}1}$ mode, the wavefront rotation direction is anti-aligned with the circular polarization. Moreover, two OAM modes composed of the same high-order vector modes have identical propagation constants, which are degenerate.

III. Coupling Between High-Order Vector Modes in the Elliptical OAM Fibers

To analyze the mode coupling between the corresponding modes in the same OAM mode group, we must resort to the high-order vector modes (HE_{l+1} and $EH_{\mathrm{l}\text{-}1}$ modes). The interactions among the vector modes of TE_{01}, TM_{01}, and HE_{21} have been studied in detail, and the results indicate that the mode coupling among these modes is serious [29]. Here, we focus on the coupling among the high-order vector modes with topological charges larger than 1. The evolution of high-order vector modes in the slightly perturbed OAM fibers satisfies the coupled mode equation [30]:

$$\frac{d\vec{A}_l(z)}{dz} = -i\left(\beta_l + K_l(z)\right)\vec{A}_l(z)$$

$$\vec{A}_l = \begin{pmatrix} a_1 \\ a_2 \\ a_3 \\ a_4 \end{pmatrix},\ \beta_l = \begin{pmatrix} \beta_{HE} & 0 & 0 & 0 \\ 0 & \beta_{HE} & 0 & 0 \\ 0 & 0 & \beta_{EH} & 0 \\ 0 & 0 & 0 & \beta_{EH} \end{pmatrix},$$

$$K_l = \begin{pmatrix} K_{11} & K_{12} & K_{13} & K_{14} \\ K_{21} & K_{22} & K_{23} & K_{24} \\ K_{31} & K_{32} & K_{33} & K_{34} \\ K_{41} & K_{42} & K_{43} & K_{43} \end{pmatrix} \tag{3}$$

where l is the topological charge, $\vec{A}_l$ is the complex amplitude vectors of these basis functions, β_l is the diagonal matrix of the propagation constants, and K_l is a 4×4 coupling matrix. When the mode-dependent loss is ignored, K_l is the Hermitian matrix, and coupling coefficient $K_{i,j}$ between the *ith* mode and the *jth* mode is given in (4):

$$K_{i,j} = \frac{\omega}{4}\int_0^{\infty}\int_0^{2\pi} E_i^* \Delta\tilde{\varepsilon} E_j r dr d\varphi = K_{j,i}^* \tag{4}$$

where ω is the angular frequency, E_i and E_j are the complete electric fields that are composed of transverse and longitudinal components of the *ith* mode and *jth* mode, respectively, and $\Delta\tilde{\varepsilon}$ is the variation in permittivity caused by perturbation. For elliptical deformation, $\Delta\tilde{\varepsilon} \approx \xi\varepsilon_0(n_{co}^2 - n_{cl}^2)\delta(r-a)\cos 2\varphi$ [30], where ξ is the deformation factor related to the deformation strength, ε_0 is the permittivity, n_{co} and n_{cl} are the refractive indices of the core and cladding, respectively, and a is the core radius. The integral calculation of the coupling coefficient $K_{i,j}$ is complex and unnecessary, but the integration over φ is very easy to obtain because the electric field expressions of E_i, E_j, and $\Delta\tilde{\varepsilon}$ depend on φ. When the integration over φ is nonzero, coupling between the corresponding modes occurs; otherwise, coupling does not appear.

Analogous to the HE_{11} mode in single-mode fibers, we calculate the coupling matrix of high-order vector modes in OAM fibers. In the single-mode fibers, the basis functions are selected as the HE_{11} modes, whose electric fields can be obtained according to (1) for *HE* with $l = 0$:

$$|HE_{11}^x\rangle \begin{pmatrix} E_x \\ E_y \\ E_z \end{pmatrix} = \begin{pmatrix} F_0(r) \\ 0 \\ iH_0(r)\cos\varphi \end{pmatrix},\ |HE_{11}^y\rangle \begin{pmatrix} E_x \\ E_y \\ E_z \end{pmatrix} = \begin{pmatrix} 0 \\ G_0(r) \\ iH_0(r)\sin\varphi \end{pmatrix} \tag{5}$$

By substituting (5) and the expression of $\Delta\tilde{\varepsilon}$ into (4), we obtain the corresponding coupling matrix K_0:

$$K_0 = \begin{pmatrix} \frac{\gamma_{11}^2\pi}{2} & 0 \\ 0 & -\frac{\gamma_{22}^2\pi}{2} \end{pmatrix} = \frac{\pi}{2}\begin{pmatrix} \gamma_{11}^2 & 0 \\ 0 & -\gamma_{22}^2 \end{pmatrix} \tag{6}$$

where, $\gamma_{11} = \xi H_0(r)/F_0(r)$, $\gamma_{22} = \xi H_0(r)/G_0(r)$. For the coupling matrix, the self-coupling coefficients (K_{11}, K_{22}) describe a mismatch of the basis functions, and the mutual coupling coefficient (K_{12}, K_{21}) describes the coupling between the different basis functions. As shown in (6), K_0 is a diagonal matrix; thus, the elliptical deformation of a single-mode fiber only introduces an effective index difference between x polarization and y polarization, but it does not cause their coupling. Therefore, the eigenmodes of elliptical single-mode fibers continue to maintain x and y polarizations of the HE_{11} mode.

In the OAM fibers, the basis functions are selected to be even and odd modes of HE_{l+1} and $EH_{l\text{-}1}$ modes, whose expressions can be obtained according to (1):

$$\begin{aligned}
\left|HE_{l+1}^{even}\right\rangle \begin{pmatrix} E_x \\ E_y \\ E_z \end{pmatrix} &= -\begin{pmatrix} F_l(r)\cos l\varphi \\ -G_l(r)\sin l\varphi \\ iH_l(r)\cos(l+1)\varphi \end{pmatrix} \\
\left|HE_{l+1}^{odd}\right\rangle \begin{pmatrix} E_x \\ E_y \\ E_z \end{pmatrix} &= -\begin{pmatrix} F_l(r)\sin l\varphi \\ G_l(r)\cos l\varphi \\ iH_l(r)\sin(l+1)\varphi \end{pmatrix} \\
\left|EH_{l-1}^{even}\right\rangle \begin{pmatrix} E_x \\ E_y \\ E_z \end{pmatrix} &= \begin{pmatrix} F_l(r)\cos l\varphi \\ G_l(r)\sin l\varphi \\ -iH_l(r)\cos(l-1)\varphi \end{pmatrix} \\
\left|EH_{l-1}^{odd}\right\rangle \begin{pmatrix} E_x \\ E_y \\ E_z \end{pmatrix} &= \begin{pmatrix} F_l(r)\sin l\varphi \\ -G_l(r)\cos l\varphi \\ -iH_l(r)\sin(l-1)\varphi \end{pmatrix}
\end{aligned} \tag{7}$$

By substituting (7) and the expression of $\Delta\tilde{\varepsilon}$ into (4), the corresponding coupling matrix K_l ($l > 1$) is obtained, which is an approximate expression for elliptical deformation:

$$K_l = \begin{pmatrix} 0 & 0 & K_{13} & 0 \\ 0 & 0 & 0 & K_{24} \\ K_{31} & 0 & 0 & 0 \\ 0 & K_{42} & 0 & 0 \end{pmatrix} \tag{8}$$

where K_{ij} depends on core ellipticity, the topological charge number, and radial-dependent function of z directions from different modes. It is difficult to obtain an analytical expression for the coupling matrix. Here, the coupling between different modes is provided qualitatively. The quantitative coupling relationship will be presented in the following simulation. The coupling matrix K_l is not a diagonal matrix, and the values of coupling coefficients K_{13}, K_{31}, K_{24} and K_{42} are not zero, which implies that mode coupling occurs between even (or odd) modes of HE_{l+1} and $EH_{l\text{-}1}$ modes. Therefore, the elliptical deformation of OAM fibers not only introduces an effective index difference between even and odd modes of high-order vector modes but also destroys the eigenmode structure. Thus, the effect of the elliptical deformation on high-order vector modes is different from that on HE_{11} modes. The reason is that the polarization state of high-order vector modes is spatially inhomogeneous [31]. Therefore, the concept of "PMD" in a single-mode fiber cannot be directly applied to OAM fibers.

By solving the eigenvectors of coupling matrix K_l, we can obtain the eigenmodes of the elliptical OAM fibers, which are no longer pure *HE* or *EH* vector modes but hybrid states of them. Thus, the eigenmodes are written as follows:

$$\begin{aligned}
em_l^1 &= \left|HE_{l+1}^{even}\right\rangle - \sigma_1\left|EH_{l-1}^{even}\right\rangle \\
&= \begin{pmatrix} -(1+\sigma_1)F_l(r)\cos l\varphi \\ (1-\sigma_1)G_l(r)\sin l\varphi \\ -iH_l(r)[\cos(l+1)\varphi - \sigma_1\cos(l-1)\varphi] \end{pmatrix} \\
em_l^2 &= \left|HE_{l+1}^{odd}\right\rangle - \sigma_2\left|EH_{l-1}^{odd}\right\rangle \\
&= \begin{pmatrix} -(1+\sigma_2)F_l(r)\sin l\varphi \\ -(1-\sigma_2)G_l(r)\cos l\varphi \\ -iH_l(r)[\sin(l+1)\varphi - \sigma_2\sin(l-1)\varphi] \end{pmatrix} \\
em_l^3 &= \left|EH_{l-1}^{even}\right\rangle + \sigma_1\left|HE_{l+1}^{even}\right\rangle \\
&= \begin{pmatrix} (1-\sigma_1)F_l(r)\cos l\varphi \\ (1+\sigma_1)G_l(r)\sin l\varphi \\ -iH_l(r)[\cos(l-1)\varphi + \sigma_1\cos(l+1)\varphi] \end{pmatrix} \\
em_l^4 &= \left|EH_{l-1}^{odd}\right\rangle + \sigma_2\left|HE_{l+1}^{odd}\right\rangle \\
&= \begin{pmatrix} (1-\sigma_2)F_l(r)\sin l\varphi \\ -(1+\sigma_2)G_l(r)\cos l\varphi \\ -iH_l(r)[\sin(l-1)\varphi + \sigma_2\sin(l+1)\varphi] \end{pmatrix}
\end{aligned} \tag{9}$$

where the first part of the constituting eigenmodes represents the dominant component, the second part represents the disturbance term which is the secondary component, and σ_j ($0 \le \sigma_j \le 1$, $j = 1, 2, 3, 4$) is the ratio of the disturbance term to the dominant component. (9) also includes the spin-orbit coupling effects. In addition, the value of σ_j depends on the elliptical deformation, and a more severe deformation has a larger σ_j. When the elliptical deformation is extremely small, σ_j is close to zero, and the eigenmodes are still high-order vector modes. When the elliptical deformation increases, σ_j increases, and the eigenmodes become a hybrid of HE_{l+1} and $EH_{l\text{-}1}$ modes. When the elliptical deformation is sufficiently large, σ_j approaches 1. In this case, the eigenmodes become LPV modes [8], which can be expressed as follows:

$$\begin{aligned}
em_l^1 &= \begin{pmatrix} F_l(r)\cos l\varphi \\ 0 \\ -iH_l(r)\sin l\varphi\sin\varphi \end{pmatrix}, \\
em_l^2 &= \begin{pmatrix} F_l(r)\sin l\varphi \\ 0 \\ iH_l(r)\cos l\varphi\sin\varphi \end{pmatrix} \\
em_l^3 &= \begin{pmatrix} 0 \\ G_l(r)\sin l\varphi \\ -iH_l(r)\cos l\varphi\cos\varphi \end{pmatrix}, \\
em_l^4 &= \begin{pmatrix} 0 \\ G_l(r)\cos l\varphi \\ iH_l(r)\sin l\varphi\cos\varphi \end{pmatrix}
\end{aligned} \tag{10}$$

Note that our goal is to qualitatively clarify the coupling relationship between high-order vector modes by the coupled mode equation and do not provide the precise coupling strength and effective index difference among different eigenmodes because of the complicated calculation, which will be evaluated by numerical analysis methods in the following.

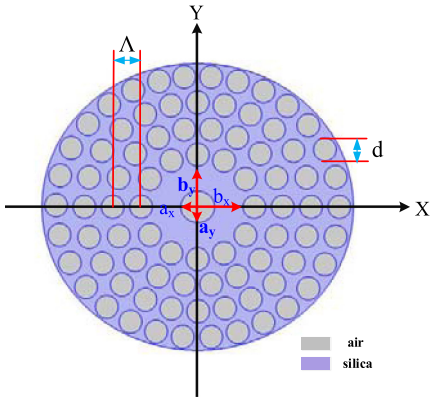

Fig. 3. Geometry structure of elliptical C-PCF.

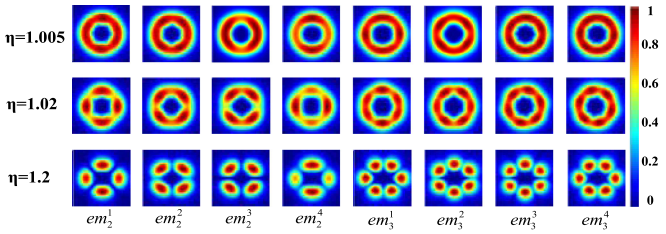

Fig. 4. Normalized intensity of eigenmodes with different ellipticities η for the C-PCF.

Compared with conventional ring-core fibers, a circular photonic crystal fiber (C-PCF) supporting OAM modes is easy to achieve the large refractive index contrast without doping and exhibits some flexibly adjustable properties [32], [33]. Moreover, C-PCF belongs to the category of ring fiber and can be equivalent to the ring-core fiber [34]. Here, we take a C-PCF as an example to analyze the structural damage of eigenmodes and the effective index difference between adjacent eigenmodes. The elliptical C-PCF is formed by removing the first two layers of air holes of the photonic crystal fiber base and arranging a large air hole in the center, as shown in Fig. 3. The refractive indices of air and silica are 1 and 1.444 (at a wavelength of 1.55 μm), respectively. Λ and d denote the concentric spacing and the diameter of cladding air holes. The inner radii along the x axis and y axis are a_x and a_y, respectively, and the outer radii along the x axis and y axis are b_x and b_y, respectively. The ratio η represents the ellipticity, where $\eta = b_x/b_y = a_x/a_y$ ($\eta = 1$ for a perfect circular ring). The fiber structure parameters are set as $\Lambda = 2.0$ μm, $d/\Lambda = 0.8$, $a_x = 1.2$ μm and $b_x = 3.2$ μm, respectively.

Fig. 4 intuitively illustrates the variation of the normalized intensity of eigenmodes with ellipticity η for the C-PCF. When η is 1.005, the eigenmodes are almost pure high-order vector modes and have a ring-shaped intensity distribution. With the increase of η, the structure of high-order vector modes is gradually destroyed, and finally the eigenmodes degrade into LPV modes. To further elucidate the effect of the elliptical deformation on the structural damage of eigenmodes, Fig. 5 shows σ of the eigenmodes as a function of η, which is obtained by finite element mode solver COMSOL [20]. σ obviously increases with increasing η, and the curves are roughly divided into three

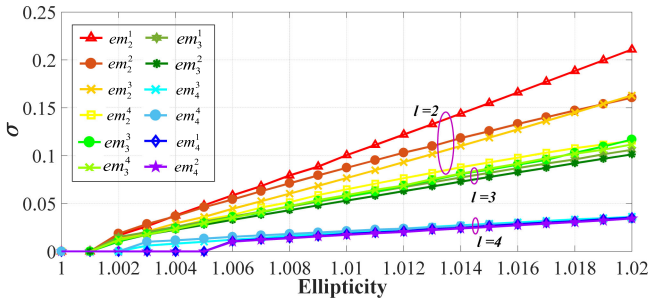

Fig. 5. σ of eigenmodes in elliptical C-PCF as a function of ellipticity η.

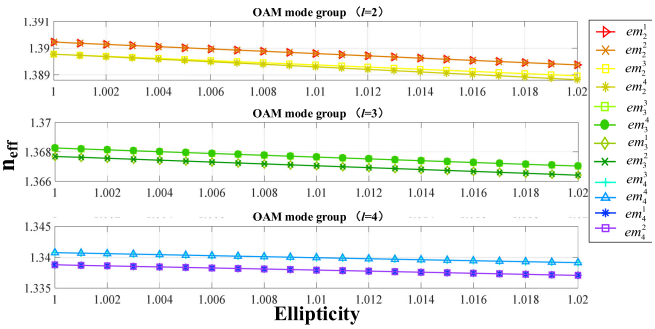

Fig. 6. Effective index n_{eff} of the eigenmodes in the C-PCF as a function of ellipticity η.

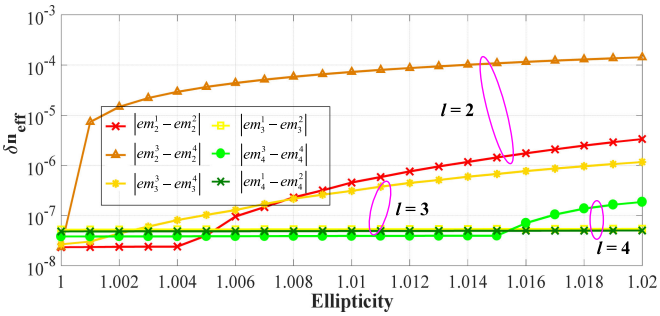

Fig. 7. Effective index difference δn_{eff} between adjacent eigenmodes in the C-PCF as a function of ellipticity η.

mode groups according to topological charge l. For a larger l carried by the eigenmode, σ of the eigenmode is smaller. For the fourth-order OAM mode group (HE_{51} and EH_{31} modes), σ is always less than 0.04 in the ellipticity range of 1-1.02. Therefore, the structure of the HE_{51} and EH_{31} modes has a large tolerance to elliptical deformation. In addition, when the ellipticity is less than 1.01, σ of all eigenmodes is less than 0.1, which implies that the corresponding purity of high-order vector modes is larger than 99%. In this case, the structural damage of high-order vector modes can be ignored. Here, the purity is defined as the power weight of the major high-order vector modes in the eigenmodes, which can be expressed as $1/(1+\sigma_i^2)$ [14].

Figs. 6 and 7 present the effective index of eigenmodes and effective index difference δn_{eff} between adjacent eigenmodes as a function of ellipticity η, respectively. As shown in Fig 6, the eigenmodes in different OAM mode groups have large effective index separation; thus, coupling among OAM modes in different

mode groups can be ignored. For the eigenmodes in the same OAM mode group, em_l^1 and em_l^2 (destroyed even and odd modes of the HE_{l+1} mode) and em_l^3 and em_l^4 (destroyed even and odd modes of the $EH_{l\text{-}1}$ mode), have similar refractive indices. Therefore, we must calculate the δn_{eff} between them. δn_{eff} between adjacent modes increases with increasing ellipticity η, and a higher order of modes corresponds to a smaller δn_{eff}, as shown in Fig. 7. δn_{eff} in the fourth-order OAM mode group always remains small in the range of ellipticity of 1-1.02, which indicates that the degeneracy of these modes is not easily broken.

In summary, when the ellipticity is relatively small (η <1.01, mode purity >99%), the elliptical deformation of OAM fibers mainly introduces δn_{eff} between even and odd high-order vector modes and the structural damage of high-order vector modes can be ignored. With the increase of ellipticity from 1.01 to 1.02, the elliptical deformation of OAM fibers not only introduces δn_{eff} between even- and odd-order vector modes, but also make the structural damage of high-order vector modes to become more and more serious, which will cause coupling between even (or odd) modes of HE_{l+1} and $EH_{l\text{-}1}$ modes.

IV. Mechanisms of OAM Mode Coupling

As described in the previous section, the effect of elliptical deformation on high-order vector modes can be roughly distinguished into two categories. The OAM modes in fibers are composed of even and odd high-order vector modes with a phase difference of π/2; thus, the coupling between OAM modes can also be divided into two cases. Note that it is inevitable that spin-orbit coupling always exists in OAM fiber. Here we focus on the influencing mechanism of elliptical deformation on OAM modes. In order to make the analysis more concise and clear, we ignore spin-orbit coupling and regard the characteristic modes in OAM fiber as ideal high-order vector modes in the following.

- *Case 1 (small ellipticity η <1.01):* The OAM modes composed of HE_{l+1} and $EH_{l\text{-}1}$ modes are independent of each other, thus can be treated separately. The effective index difference δn_{eff} between even and odd modes of the high-order vector modes destroys the mode stability, which causes coupling between two OAM modes composed of the same high-order vector mode. In this case, the OAM mode coupling is similar to the PMD phenomenon in single-mode fibers.
- *Case 2 (large ellipticity 1.01 < η <1.02):* The OAM modes composed of HE_{l+1} and $EH_{l\text{-}1}$ modes are not independent of each other. Apart from the coupling between two OAM modes composed of the same vector mode, coupling also occurs between two OAM modes superposed by HE_{l+1} and $EH_{l\text{-}1}$ modes.

A. OAM Mode Coupling Caused By Small Ellipticity

The OAM modes in fibers are defined as a superposition of even and odd modes from the same high-order vector modes with a phase difference of π/2. In an ideal OAM fiber, even and odd modes from the same vector mode have identical effective indices. Therefore, there is no time delay difference between them, and the OAM modes can stably exist in fibers.

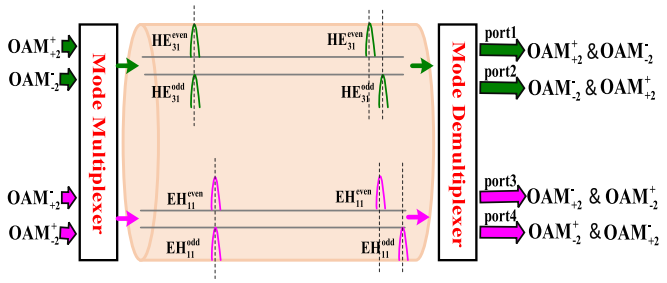

Fig. 8. Schematic diagram of the OAM mode coupling caused by a small ellipticity.

In fibers with a small ellipticity, the degeneracy of even and odd high-order vector modes is broken. The time delay difference increases with increasing transmission distance, which will correspondingly destroy the stability of OAM modes and cause coupling between two OAM modes composed of the same high-order vector modes. We take the second OAM mode group ($l = 2$) as an example to elucidate the OAM mode coupling mechanism, as shown in Fig. 8.

When the eigenmode HE_{31} (EH_{11}) is transmitted in the OAM fibers, phase difference θ between even and odd modes can be expressed as follows:

$$\theta = \frac{2\pi}{\lambda}\delta n_{eff} L \tag{11}$$

where λ is the operating wavelength, δn_{eff} is the effective index difference between even and odd modes of the same vector modes, and L is the transmission distance. The synthesized mode ψ_1 can be written as follows:

$$\psi_1(\varphi) = HE_{31}^{even} + i\exp(i\theta)\, HE_{31}^{odd} \tag{12}$$

In addition, ψ_1 can be represented as a superposition of all pure OAM modes in the fiber [35]:

$$\psi_1(\varphi) = \sum_{l=-\infty}^{+\infty} A_l \exp(il\varphi) \tag{13}$$

where A_l is the proportionality coefficient of the pure OAM mode:

$$A_l = \frac{1}{2\pi}\int_{-\pi}^{\pi} \psi_1(\varphi)\exp(-il\varphi)\, d\varphi \tag{14}$$

By substituting (12) into (14), we obtain the proportionality coefficient of each OAM mode as a function of θ, as shown in Fig. 9. The two OAM modes (OAM_{+2}^{+} and OAM_{-2}^{-}) formed by even and odd modes of the HE_{31} mode couple to each other with increasing phase difference θ and show a periodicity. Here only a small section of OAM fiber with constant birefringence direction is represented. Therefore, the periodic behavior is due to neglecting the randomness of orientation rotation along fiber transmission distance.

Fig. 10 shows the normalized intensity, phase and polarization of the synthesized mode at points (a)-(f) in Fig. 9. To better understand the phase variation of the mode, the third row exhibits the phase distribution of the mode at a certain radius. The intensity is obviously always evenly distributed along the

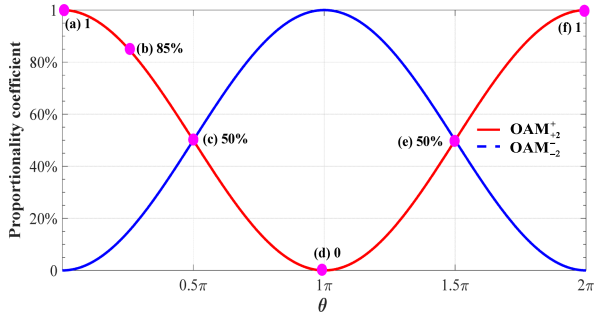

Fig. 9. Proportionality coefficient of OAM modes as a function of θ. (a) $\theta = 0$. (b) $\theta = \pi/4$. (c) $\theta = \pi/2$. (d) $\theta = \pi$. (e) $\theta = 3\pi/2$. (f) $\theta = 2\pi$.

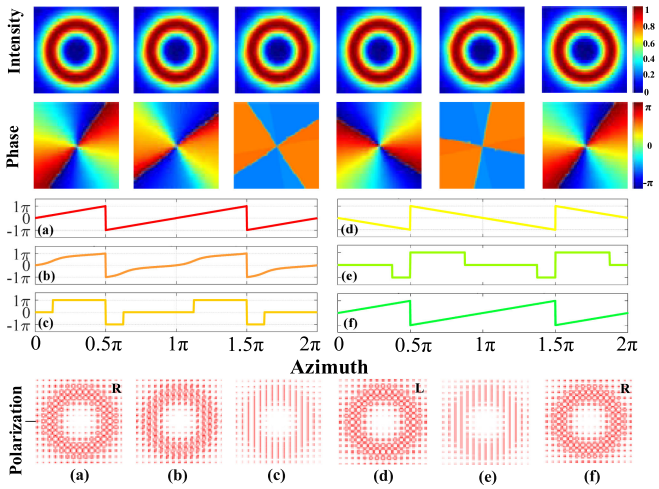

Fig. 10. Intensity, phase and polarization of the synthesized modes as a function of θ. (a) $\theta = 0$. (b) $\theta = \pi/4$. (c) $\theta = \pi/2$. (d) $\theta = \pi$. (e) $\theta = 3\pi/2$. (f) $\theta = 2\pi$.

azimuth at each value of θ, while the phase and polarization vary with θ and take on a periodic trend. With increasing θ, the helical phase wavefront of OAM modes is gradually destroyed; when θ is π, the wavefront is reversed. When θ becomes 2π, the phase changes complete a cycle and return to the initial state. The polarization also experiences a similar process to the phase wavefront: it changes from right circular polarization ($\theta = 0$) to linear polarization ($\theta = \pi/2$), to left circular polarization ($\theta = \pi$), and subsequently back to the right circular polarization (initial state) [36]. Compared to the OAM modes in the ideal OAM fiber (Fig. 1), this type of mode coupling will destroy the polarization and phase of OAM modes, and its effect on the phase and polarization is consistent. In addition, the OAM fiber exhibits a mode field evolution similar to that of weakly-guiding fiber with small ellipticity, that is, the elliptical deformation changes the polarization and OAM of the OAM modes without changing the intensity distribution of the modes [37]–[41].

B. OAM Mode Coupling Caused By Large Ellipticity

For OAM fibers with a large ellipticity, the OAM modes composed of HE_{l+1} and EH_{l-1} modes are not independent of each other. We also take the second OAM mode group as an example to illustrate the OAM mode coupling mechanism, as

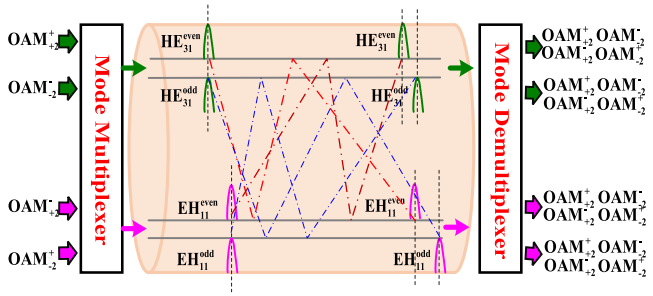

Fig. 11. Schematic diagram of OAM mode coupling caused by large ellipticity.

shown in Fig. 11. The four OAM modes in the same mode group are injected into the fiber, which will excite the HE_{31} and EH_{11} modes. Since the eigenmodes of the large-ellipticity OAM fibers are hybrid modes of HE_{31} and EH_{11} modes, the HE_{31} and EH_{11} modes cannot stably exist in the fiber. There may be leakage between even (or odd) modes of HE_{31} and EH_{11} modes, which will cause coupling among the corresponding OAM modes. Therefore, in OAM fibers with large ellipticity, coupling occurs among four OAM modes in the same OAM mode group.

When the optical field travels through OAM fibers with large ellipticity, the synthesized modes in the same OAM mode group can be expressed as follows:

$$\begin{aligned}
OAM^{1}_{synthesized} &= em^{1}_{l} + i\exp(i\theta)em^{2}_{l} \\
&= \left(HE^{even}_{l+1} + i\exp(i\theta)HE^{odd}_{l+1}\right) \\
&\quad - \tilde{\sigma}_{12}\left(EH^{even}_{l-1} + i\exp(i\theta)EH^{odd}_{l-1}\right) \\
OAM^{2}_{synthesized} &= em^{1}_{l} - i\exp(i\theta)em^{2}_{l} \\
&= \left(HE^{even}_{l+1} - i\exp(i\theta)HE^{odd}_{l+1}\right) \\
&\quad - \tilde{\sigma}_{12}\left(EH^{even}_{l-1} - i\exp(i\theta)EH^{odd}_{l-1}\right) \\
OAM^{3}_{synthesized} &= em^{3}_{l} + i\exp(i\theta)em^{4}_{l} \\
&= \left(EH^{even}_{l-1} + i\exp(i\theta)EH^{odd}_{l-1}\right) \\
&\quad + \tilde{\sigma}_{12}\left(HE^{even}_{l+1} + i\exp(i\theta)HE^{odd}_{l+1}\right) \\
OAM^{4}_{synthesized} &= em^{3}_{l} - i\exp(i\theta)em^{4}_{l} \\
&= \left(EH^{even}_{l-1} - i\exp(i\theta)EH^{odd}_{l-1}\right) \\
&\quad + \tilde{\sigma}_{12}\left(HE^{even}_{l+1} - i\exp(i\theta)HE^{odd}_{l+1}\right)
\end{aligned} \tag{15}$$

where $\tilde{\sigma}_{12}$ is the average values of σ_1 and σ_2, and their size depends on the structural damage degree of the eigenmodes. The first item of the synthesized modes represents the superposition of two OAM modes composed of even and odd modes from the same high-order vector mode, which is the dominant component of the mode coupling. The second item represents the contribution from adjacent OAM mode pairs, which is a secondary component of the mode coupling. In OAM fibers with a large ellipticity, coupling obviously occurs among four OAM modes in the same OAM mode group, and the coupling between two

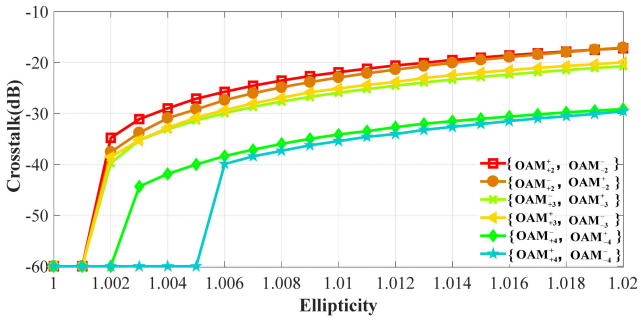

Fig. 12. Crosstalk of OAM modes as a function of ellipticity η.

OAM modes composed of the same high-order vector mode is also more serious. When the mode coupling between adjacent OAM mode pairs can be ignored, the mode demultiplexer is followed by two isolated receivers: one for OAM_{+l}^{+} and OAM_{-l}^{-} modes (composed of HE_{l+1} modes) and the other for $OAM_{+l}^{-}$and OAM_{-l}^{+} modes (composed of $EH_{l\text{-}1}$ modes). If the adjacent mode coupling is not negligible, a 4×4 MIMO digital signal processing system is required. To understand the effect of the elliptical deformation on the mode coupling between OAM modes constituted by HE_{l+1} and $EH_{l\text{-}1}$ modes, the crosstalk of OAM modes as a function of ellipticity η is shown in Fig. 12. Here, the crosstalk is defined as the power leakage between adjacent OAM mode pairs $OAM_{\pm l}^{\pm}$ and $OAM_{\pm l}^{\mp}$ modes:

$$Crosstalk\ on\ OAM_{\pm l}^{\pm} = 10\log\left(\frac{power_{OAM_{\pm l}^{\mp}}}{power_{OAM_{\pm l}^{\pm}} + power_{OAM_{\pm l}^{\mp}}}\right) \quad (16)$$

where $power_{OAM_{\pm l}^{\pm}}$ is the power of OAM mode pair $OAM_{\pm l}^{\pm}$, and $power_{OAM_{\pm l}^{\mp}}$ is the power of adjacent OAM mode pair $OAM_{\pm l}^{\mp}$. As shown in Fig. 12, the crosstalk of OAM modes gradually increases with ellipticity η, and a larger topological charge l carried by the OAM mode corresponds to a smaller crosstalk of OAM modes. For η of 1-1.013, the crosstalk of all OAM modes is less than 20 dB (the mode purity is larger than 99%); thus, the mode coupling between OAM modes constituted by HE_{l+1} and $EH_{l\text{-}1}$ modes can be ignored. When η is larger than 1.013, the coupling between adjacent OAM mode pairs cannot be ignored.

V. Conclusion

In this paper, the intramode-group coupling effects in elliptical deformation OAM fibers were examined using coupling mode theory and numerical simulation. The elliptical deformation of OAM fibers not only introduces a time delay difference between even and odd modes of high-order vector modes of the same mode group but also destroys the structure of high-order vector modes; the degree of structural damage depends on the strength of the elliptical deformation. For OAM fibers with small ellipticity ($0 < \eta < 1.01$), the structural damage of high-order vector modes can be ignored; hence, the elliptical deformation only introduces a time delay difference between even and odd modes. For this scenario, when the optical field travels through the OAM fiber, the time delay difference between even and odd modes increases with the transmission distance, which will cause a coupling between two OAM modes composed of the same high-order vector mode. This coupling mechanism is similar to the PMD phenomenon in single-mode fibers. In OAM fibers with large ellipticity ($1.01 < \eta < 1.02$), the structural damage of high-order vector modes cannot be ignored. The eigenmodes of fibers are no longer HE_{l+1} or $EH_{l\text{-}1}$ modes but a hybrid of HE_{l+1} and $EH_{l\text{-}1}$ modes. For this case, coupling occurs among four OAM modes from the same OAM mode group, and the coupling between two OAM modes composed of the same high-order vector mode is also more serious.

Our research has revealed the coupling mechanism of OAM modes in depth, which paves the way for the establishment of accurate propagation models and provides a theoretical basis for designing OAM fibers with better performance. In addition, we only analyzed the mode coupling caused by elliptical deformation, and other forms of perturbations can be similarly analyzed.

References

[1] D. J. Richardson, J. M. Fini, and L. E. Nelson, "Space-division multiplexing in optical fibres," *Nat. Photon.*, vol. 7, no. 5, pp. 354–362, May 2013.
[2] G. Li, N. Bai, N. Zhao, and C. Xia, "Space-division multiplexing: The next frontier in optical communication," *Adv. Opt. Photon.*, vol. 6, no. 4, pp. 413–487, Dec. 2014.
[3] P. Sillard and M. Bigot-Astruc, and D. Molin, "Few-mode fibers for mode-division-multiplexed systems," *J. Lightw. Technol.*, vol. 32, no. 16, pp. 2824–2829, Aug. 2014.
[4] H. Zhang, M. Bigot-Astruc, L. Bigot, P. Sillard, and J. Fatome, "Multiple modal and wavelength conversion process of a 10-Gbit/s signal in a 6-LP-mode fiber," *Opt. Exp.*, vol. 27, no. 11, pp. 15413–15425, May. 2019.
[5] M. Nakazawa, M. Yoshida, and T. Hirooka, "Measurement of mode coupling distribution along a few-mode fiber using a synchronous multi-channel OTDR," *Opt. Exp.*, vol. 22, no. 25, pp. 31299–31309, Mar. 2014.
[6] R. Zhang *et al.*, "Utilizing adaptive optics to mitigate intra-modal-group power coupling of graded-index few-mode fiber in a 200-gbit/s mode-division-multiplexed link," *Opt. Lett.*, vol. 45, no. 13, pp. 3577–3580, Jul. 2020.
[7] T. Mori, T. Sakamoto, M. Wada, T. Yamamoto, and F. Yamamoto, "Few-mode fibers supporting more than two LP modes for mode-division-multiplexed transmission with MIMO DSP," *J. Lightw. Technol.*, vol. 32, no. 14, pp. 2468–2479, Jul. 2014.
[8] L. Wang and S. LaRochelle, "Design of eight-mode polarization-maintaining few-mode fiber for multiple-input multiple-output-free spatial division multiplexing," *Opt. Lett.*, vol. 40, no. 24, pp. 5846–5849, Dec. 2015.
[9] L. Wang *et al.*, "Linearly polarized vector modes: Enabling MIMO-free mode-division multiplexing," *Opt. Exp.*, vol. 25, no. 10, pp. 11736–11748, May. 2017.
[10] C. Brunet, P. Vaity, Y. Messaddeq, S. Larochelle, and L. Rusch, "Design, fabrication and validation of an OAM fiber supporting 36 states," *Opt. Exp.*, vol. 22, no. 21, pp. 26117–26127, Oct. 2014.
[11] S. Chen, S. Li, L. Fang, A. Wang, and J. Wang, "OAM mode multiplexing in weakly guiding ring-core fiber with simplified MIMO-DSP," *Opt. Exp.*, vol. 27, no. 26, pp. 38049–38060, Dec. 2019.
[12] J. Zhang *et al.*, "Mode division multiplexed transmission of WDM signals over 100-km single-span oam fiber," *Photon. Res.*, vol. 8, no. 7, pp. 1236–1242, Jul. 2020.
[13] S. Golowich, "Asymptotic theory of strong spin-orbit coupling in optical fiber," *Opt. Lett.*, vol. 39, no. 1, pp. 92–95, Jan. 2014.
[14] Z. zhang *et al.*, "Optical fiber design with orbital angular momentum light purity higher than 99.9%," *Opt. Exp.*, vol. 23, no. 23, pp. 29331–29341, Nov. 2015.
[15] Y. Yue *et al.*, "Mode properties and propagation effects of optical orbital angular momentum (OAM) modes in a ring fiber," *IEEE Photon. J.,* vol. 4, no. 2, pp. 535–543, Apr. 2014.

[16] L. Wang, P. Vaity, S. Chatigny, Y. Messaddeq, L. A. Rusch, and S. Larochelle, "Orbital-angular-momentum polarization mode dispersion in optical fibers," *J. Lightw. Technol.*, vol. 34, no. 8, pp. 1661–1671, Dec. 2016.
[17] J. Zhou *et al.*, "Performance analyses of LDPC-coded orbital angular momentum (OAM) optical communications in a multi-bending ring fiber," in *Proc. Asia Commun. Photon. Conf.*, 2014, pp. 1–3.
[18] H. Yan *et al.*, "Deformation of orbital angular momentum modes in bending ring-core fiber," *Chin. Opt. Lett.*, vol. 15, no. 3, pp. 55–59, Mar. 2017.
[19] Z. Ma, G. Prabhakar, P. Gregg, and S. Ramachandran, "Robustness of OAM fiber modes to geometric perturbations," in *Proc. Las. Elect.-Opt. Conf.*, 2018, pp. 1–2.
[20] B. Zhang *et al.*, "Theory for mode coupling in perturbed fibers," *Opt. Commun.*, vol. 463, no. 125355, pp. 1–12, May 2020.
[21] R. Bhandari, "Analytic expressions for orbital angular momentum modal crosstalk in a slightly elliptical fiber," *IEEE Photon. J.*, vol. 12, Dec. 2020, Art. no. 7202621.
[22] B. Charles, U. Bora, L. Wang, Y. Messaddeq, L. A. Rusch, and S. Larochelle, "Design of a family of ring-core fibers for OAM transmission studies," *Opt. Exp.,* vol. 23, no. 8, pp. 10553–10563, Apr. 2015.
[23] G. Guerra, M. Lonardi, A. Galtarossa, L. A. Rusch, A. Bononi, and L. Palmieri, "Analysis of modal coupling due to birefringence and ellipticity in strongly guiding ring-core OAM fibers," *Opt. Exp.,* vol. 27, no. 6, pp. 8308–8326, Mar. 2019.
[24] M. Lonardi *et al.*, "Mode coupling analysis of hollow ring-core fibers for oam transmission," in *Proc. Eur. Conf. Opt. Commun.*, 2017, pp. 1–3.
[25] G. Guerra, A. Galtarossa, and L. Palmieri, "Numerical analysis of power coupling in few-mode step index fibers," in *Proc. Opt. Fiber Commun. Conf.*, 2018, pp. 1–3.
[26] L. Palmieri and A. Galtarossa, "Intramodal dispersion properties of step-index few-mode spun fibers," *J. Lightw. Technol.*, vol. 34, no. 2, pp. 303–313, Dec. 2016.
[27] M. Banawan, L. Wang, S. LaRochelle, and L. A. Rusch, "Quantifying the coupling and degeneracy of OAM modes in high-index-contrast ring core fiber," *J. Lightw. Technol.*, vol. 39, no. 2, pp. 600–611, Jan. 2021.
[28] A. W. Snyder and J. Love, "Optical waveguide theory," in *Science Paperbacks*, Boston, MA, USA: Springer, 1983.
[29] R. M. Nejad, L. Wang, J. Lin, S. LaRochelle, and L. A. Rusch, "The impact of modal interactions on receiver complexity in OAM fibers," *J. Lightw. Technol.*, vol. 35, no. 21, pp. 4692–4699, Sep. 2017.
[30] L. Palmieri and A. Galtarossa, "Coupling effects among degenerate modes in multimode optical fibers," *IEEE Photon. J.,* vol. 6, no. 6, pp. 1–8, Dec. 2014, Art. no. 0600408.
[31] S. Chen, X. Zhou, Y. Liu, X. Ling, and H. Luo, "Generation of arbitrary cylindrical vector beams on the higher order poincare´sphere," *Opt. Lett.*, vol. 39, no. 18, pp. 5274–5276, Jul. 2014.
[32] H. Zhang, W. Zhang, L. Xia, X. Tang, X. Zhang, and X. Zhang, "A new type circular photonic crystal fiber for orbital angular momentum mode transmission," *IEEE Photon. Technol. Lett.*, vol. 28, no. 13, pp. 1426–1429, Jun. 2016.
[33] H. Zhang *et al.*, "A design strategy of the circular photonic crystal fiber supporting good quality orbital angular momentum mode transmission," *Opt. Commun.*, vol. 397, pp. 59–66, Mar. 2017.
[34] H. Li *et al.*, "Design tool for circular photonic crystal fibers supporting orbital angular momentum modes," *Appl. Opt.*, vol. 57, no. 10, pp. 2474–2481, Apr. 2018.
[35] B. Jack, M. J. Padgett, and S. Franke-Arnold, "Angular diffraction," *New J. Phys.*, vol. 10, no. 10, pp. 6456–6460, Oct. 2008.
[36] H. Li *et al.*, "Analysis of intra-mode-group mode coupling due to ellipticity in OAM fibers," in *Proc. Asia Commun. Photon. Conf.*, 2019, pp. 1–3.
[37] C. N. Alexeyev, M. S. Soskin, and A. V. Volyar, "Spin-orbit interaction in a generic vortex field transmitted through an elliptic fiber," *Semicond. Phys. Quant.*, vol. 3, no. 4, pp. 501–513, Dec. 2000.
[38] C. N. Alexeyev, A. V. Volyar, and M. A. Yavorsky, "Transformation of optical vortices in elliptical and anisotropic optical fibres," *J. Opt. A: Pure Appl. Opt.*, vol. 9, pp. 387–394, Mar. 2007.
[39] C. N. Alexeyev, A. N. Alexeyev, B. P. Lapin, and M. A. Yavorsky, "Optical angular momentum and mode conversion in optical fibres with competing form and material anisotropy," *J. Opt. A: Pure Appl. Opt.*, vol. 10, Apr. 2008, Art. no. 055009.
[40] C. N. Alexeyev, A. N. Alexeyev, B. P. Lapin, and M. A. Yavorsky, "Controlling the optical angular momentum by elliptical anisotropic fibres," *J. Opt. A: Pure Appl. Opt.*, vol. 11, Aug. 2009, Art. no. 105406.
[41] K. N. Alekseev, A. V. Volyar, and T. A. Fadeeva, "Spin-orbit interaction and evolution of optical eddies in perturbed weakly directing optical fibers," *Opt. Spectrosc.*, vol. 93, no. 4, pp. 588–597, Oct. 2002.